



## OPEN

## SUBJECT AREAS:

METAMATERIALS  
NANOPHOTONICS AND  
PLASMONICS  
INORGANIC LEDs  
IMAGING AND SENSING

Received

24 June 2013

Accepted

21 August 2013

Published

6 September 2013

Correspondence and  
requests for materials  
should be addressed to  
T.L. (taoli@nju.edu.cn)

# Active display and encoding by integrated plasmonic polarizer on light-emitting-diode

L. Wang<sup>1</sup>, T. Li<sup>1</sup>, R. Y. Guo<sup>1</sup>, W. Xia<sup>2</sup>, X. G. Xu<sup>2</sup> & S. N. Zhu<sup>1</sup><sup>1</sup>National Laboratory of Solid State Microstructures, School of Physics, College of Engineering and Applied Sciences, Nanjing University, Nanjing 210093, China, <sup>2</sup>State Key Laboratory of Crystal Materials, Shandong University, Jinan 250100, China.

**An electrical pumped microscopic active display with integration of plasmonic polarizer and light-emitting-diode is proposed. Thanks to the strong polarized emission through the rectangular nanoholes, well designed pixels with respect to different polarizations are engineered, which give rise to flexible and controllable active display. As results, polarization multiplexed letter encoding, single and double gray-scale images and animation movies are successfully realized. Our results demonstrate a new strategy in electro-optical integration and indicate potential applications in designing new type of microscopic electro-optical devices.**

Extraordinary optical transmission (EOT) through subwavelength nanohole array in metal film has sparked tremendous research interest owing to its intriguing physics<sup>1–3</sup> and fascinating applications (e.g., color sorting<sup>4</sup>, filter<sup>5</sup>). Actually, shape resonance of localized surface plasmon (LSP) in symmetry-broken holes (e.g., rectangular hole) that gives rise to a significant polarization control also has arrested great attention<sup>6–8</sup>, in which the LSP is considered contributing to a polarized EOT in combination with the periodicity modulated surface plasmon polariton (SPP). Optical polarization rotator and converters were proposed successively based on the related EOT structural designs<sup>9–11</sup>. In fact, plasmonic polarizer has demonstrated its attractive features in recent years, for examples, in polarimetric imaging<sup>4</sup>, active color filter<sup>5,12</sup>, and high resolution color printer<sup>13</sup>. On the other side, light emitting diode (LED) is playing a more and more important role in solid state lighting and display applications due to its convenience and energy saving. However, its polarization functionality based on novel nanostructures is not fully explored. Thanks to the strong modulation of plasmonic polarizer in nano-scale, it is quite reasonable to exploit a compact integration between LED and metallic EOT structures for active polarization-resolved display.

Although there have been a number of attempts trying to adopt plasmonic structures to improve the light emission efficiency in LED system<sup>14–16</sup>, positive result was seldom reported in real electrically pumped LED devices, which is mainly due to the large metallic loss that cancels out the gain from the extracted total reflection. In this regard, we will not emphasize on the light extraction efficiency in our study, though it will be considered to some extent with a proper optimization of the structure. In this work, we developed an integrated electro-plasmonic display device with a spatially distributed EOT polarizer on GaAs based LED chip<sup>17</sup> that is electrically pumped. With careful designs of the plasmonic polarizer, active encodings and displays are realized based on the polarization resolved pixels, exhibiting the functionality of polarization division multiplexing (PDM). As examples, polarization tuned active letter encoding, images, and animation movies are demonstrated.

## Results

The EOT structure with rectangular unit holes that can work as strong polarizer has been intensively studied<sup>6,8</sup>. There are two major factors that influence the transmission spectroscopy, the lattice period and the hole shape. In the case of rectangular hole array, the aspect ratio will dominate the polarization property of the transmission light<sup>6,8</sup>. In ideal condition, only the illumination with polarization perpendicular to the long axis can be strongly transmitted. In this consideration, every rectangular unit can act as a polarization sensitive pixel that would possibly construct a complex display. Figure 1(a) intuitively shows our design scheme, in which electrically pumped LED is defined as a substrate and covered by a silver film with well-designed rectangle holes array inside. Each pixel corresponds to a polarized emitter that can be modified by hole size ( $a$  and  $b$  for long and short

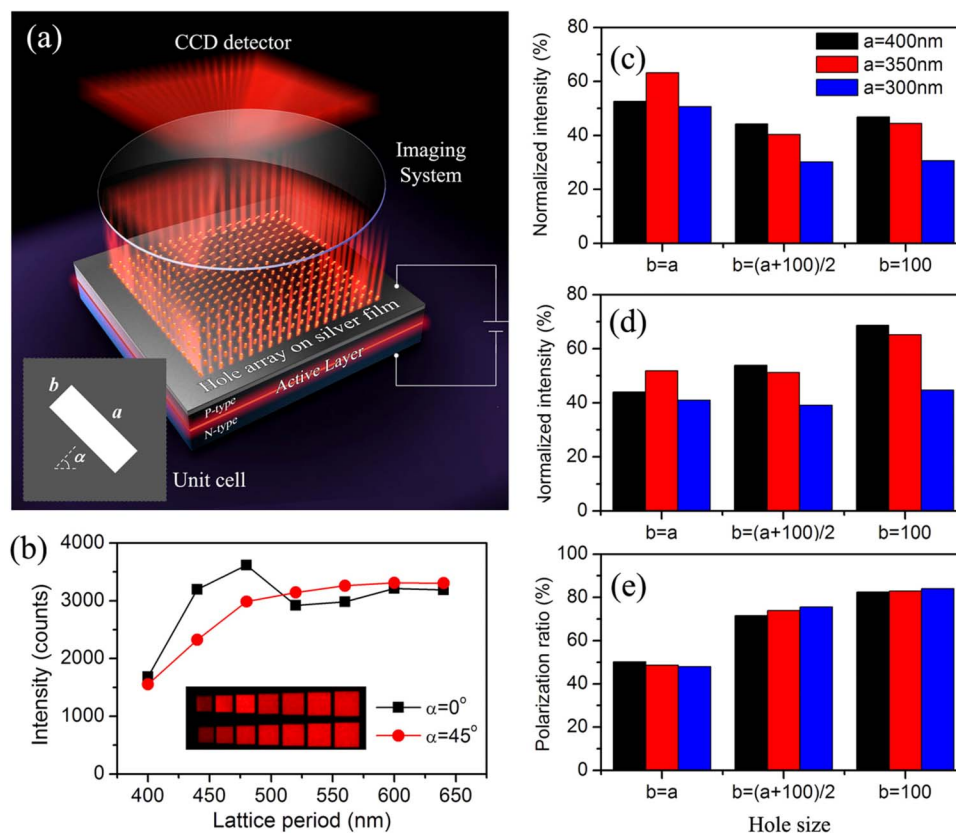


**Figure 1 | Plasmon assisted LED device and emission performance.** (a) Schematic of electrically pumped LED illumination covered with EOT structure, where inset image marks out the unit cell of rectangular hole array. (b) Illumination intensity of the two series of samples with respect to different lattice period (hole orientations are  $0^\circ$  and  $45^\circ$ , respectively). (c) Normalized total emission intensity, (d) polarized intensity (along short axis), and (e) polarization ratio of a series samples with fixed lattice period of 480 nm, while different  $a$  and  $b$  parameters.

sides respectively) and orientation (defined by angle  $\alpha$ ), shown in the inset in Fig. 1(a). With carefully designed structural parameters, active LED displays will be achieved by checking its polarization in a highly controllable way.

**Optimization of structural parameters.** Before getting into the major part of the polarization control, we would like to firstly investigate the illumination intensity with respect to the hole array parameters. Since the LED is a dispersive illumination with a wide range incident angles, it brings great difficulties to precisely analyze the transmission spectroscopy as previous studies with definite incidences<sup>1–3,6–8</sup>. To get an overall guideline to demonstrate our design, however, we experimentally investigated a number of samples with different structural parameters to obtain a certain optimum one in balancing the emission intensity and strong polarization. First, we would show the influence of the lattice period ( $P$  varies from 400 nm to 640 nm) on the emission intensity with respect to two kinds of hole orientations ( $\alpha=0^\circ$  and  $45^\circ$ ), as show in Fig. 1(b). Here, the unit holes of all samples are designed with same aspect ratio ( $a:b=3:1$ ) and occupation ratio (area of hole over the unit cell,  $\eta\sim 0.155$ ), (e.g.,  $a=300$  nm and  $b=100$  nm for the sample of  $P=440$  nm). There is strongest emission at the  $P=480$  nm for the  $\alpha=0^\circ$  case and it is also strong enough for the  $\alpha=45^\circ$  one, whose emission pictures are shown in the inset in Fig. 1(b). Therefore the lattice period of 480 nm is selected for further analyses.

Figure 1(c) depicts the emission intensities of a series of samples with different size of  $a$  and  $b$ , which has been normalized to the intensity of a blank sample (a big hole with same sample area). It is evident that the bigger hole, the stronger emission (except the sample of  $a=400$  nm, which may due to some collapse of the structure in

this large hole case). However, by checking the polarization (perpendicular to the long side of hole), we find the high aspect ratio ones (with smaller  $b$  value) have strong emissions (highest transmittance reaches  $\sim 68\%$ ) as shown in Fig. 1(d). Moreover, considering the almost non-polarized emission of bare LED, we obtained the polarization ratio of these samples by evaluating  $PR = T_{\text{pol-y}} / (T_{\text{pol-y}} + T_{\text{pol-x}})$ , as shown in Fig. 1(e). It is clear that samples with smaller  $b$  value reveal high polarization ratio (up to 80%), indicating a nearly linear polarization. Therefore, we decide to use these optimized parameters for further detailed investigations: the lattice period is 480 nm and the hole size is  $350 \times 100$  nm<sup>2</sup>. In this case the sample shows both higher power efficiency (more than two third) and stronger polarization ( $PR\sim 83\%$ ). To be noted, this group of relatively optimized parameters is not the absolute value after an exhaustion method, it only provides a guideline for further demonstration of polarization tuned encoding and displays.

**Binary letter encoding.** Since the polarization can be figured out using the rectangular hole, the LED illumination is able to carry a spatially distributed binary signal as every unit is specially designed. So it would be a kind of polarization encoding with respect to two orthogonal states, which can be decoded by switching the external polarizer in detection. Specifically, pixels constructed by nanoholes are designed into three types: H-type (bright pixel checked in horizontal polarizer), V-type (bright in vertical) and C-type (bright in both cases). In this consideration, a minimum four units are combined together to work as a “super-pixel” with arrangements depicted in Fig. 2(a), according to the principle that the hole can only be lighted by polarization perpendicular to the long side due to the strong LSP resonance. It should be noted that the short side of hole also have contributions in the case of polarization along the long

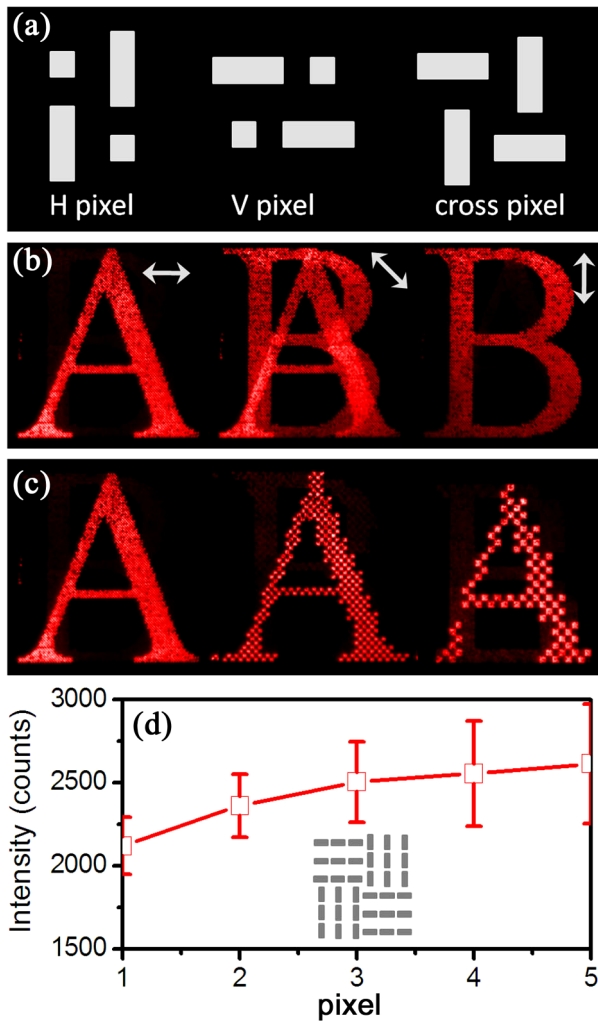


**Figure 2 | Binary image display for letter encoding.** (a) Sketch of three types of pixels composed of rectangular and square nano holes. (b) Microscope imaged Letter encoding with different polarization analyses. (c) Letter encodings by different number of pixels:  $1 \times 1$ ,  $3 \times 3$ ,  $5 \times 5$  (from left to right). (d) Emission intensity of the cross pixel with respect to different pixel index.

side, although it is minor. Then, to eliminate the illumination contrast between the C-pixel with H- and V-pixels, small square holes are added in the H- and V-type designs, whose size equals to the short side of the rectangular hole, to balance the intensity difference in polarized illuminations. With this design, we successfully generate multiplexed capital letters “A” and “B”, which can be decoded by checking polarization in H and V states respectively, as shown in Fig. 2(b) (see supplemental online material Media 1).

As has been illustrated, although LSP of shape resonance dominate the illumination intensity, the non-local SPP still contribute to a certain extent. To verify this, we intentionally expand the pixel by introducing more units (e.g., a pixel of  $3 \times 3$  units shown in inset image of Fig. 2(d)), so that the contribution of non-local SPP will increase. Figure 2(c) displays the results of pixels of  $1 \times 1$ ,  $3 \times 3$  and  $5 \times 5$  units for comparing their brightness. It is observed that the emission intensity is really enhanced as the pixels are expanded. This intensity evolution is more clearly manifested by the extracted data shown in Fig. 2(d). By expanding the pixel to  $5 \times 5$ , the intensity increases about 24%, which evidently reveals the contribution of SPP. Due to the finite propagation of SPP, the enhancement of intensity tends to be saturated by further enlarging the sub-pixel, as indicated

in Fig. 2(d). Along with this improved illumination, on the contrary, enlarging pixel will inevitably lowers down the image resolution. In practical applications, there may be a trade-off between these two factors. Nevertheless, our results do provide an instruction for a proper choice for particular usage. Moreover, this binary Letter encoding does provide us a method for the polarization-division multiplexing (PDM), which is of great possibility to be adopted in the optical communication systems.

**Gray scale image display.** In order to carry more information, we further develop our design to display gray scale images with the pixel brightness changing continuously in a certain polarization. Therefore, we step out from previous binary pixel design to an arbitrary distribution of the hole orientations. For simplification, we would like to use the pixel of  $1 \times 1$  unit for demonstration, though it can be optimized by expanding the pixel to improve the brightness. According to the LSP enhanced transmission of rectangular hole with respect to different polarizations, we would like to neglect the contribution of short side of the hole, and obtain an approximate expression of the polarized intensity as

$$I(x,y) = I_0 \cos^2(\varphi - \alpha(x,y)), \quad (1)$$

where  $\varphi$  is the checked polarization,  $\alpha$  is the hole orientation, and  $I_0$  is the maximum intensity as  $\varphi = \alpha$  or  $\alpha + \pi$ . With an defined intensity distribution  $I(x,y)$ , we can easily obtain the distribution of the hole orientation as

$$\alpha(x,y) = \frac{1}{2} \arccos\left(\frac{2I(x,y)}{I_0} - 1\right). \quad (2)$$

Therefore, we can numerically retrieve the distribution of hole orientation within the array according to a defined gray scale image. Here, we present a result of experimentally achieved image of Lena, which is commonly used as a standard test image<sup>13</sup>. Figure 3(a) displays the LED image without checking the polarization, which almost reveals a homogenous emission. While by checking the polarization in horizontal direction, Lena’s portrait is clearly manifested, as shown in Fig. 3(b). Figure 3(e) further presents the hole array design of the “eye” part, where continuous distribution of hole orientation is seen. In this stage, a single gray-scale image with respect to H-polarization is well achieved.

Moreover, this gray-scale image design can be further developed for two multiplexed images by adopting the modulation of the local pixel intensities. Actually, the polarized emission intensity of every local pixel  $I(x,y)$  can be tuned by the hole size and orientation. Defining  $u(x,y)$  as the non-polarized local pixel intensity, which is mainly determined by the hole size (here the aspect ratio is fixed at 3.5:1), we have

$$I(x,y) = u(x,y) \cos^2(\varphi - \alpha(x,y)). \quad (3)$$

By adopting  $\varphi_1 = 0$  and  $\varphi_2 = \pi/2$ , Eq. (3) is transferred to

$$\begin{cases} I_1(x,y) = u(x,y) \cos^2 \alpha \\ I_2(x,y) = u(x,y) \sin^2 \alpha \end{cases}, \quad (4)$$

where  $I_1(x,y)$  and  $I_2(x,y)$  correspond to the intensity distribution of two independent images. With Eq. (4) we can retrieve the distributions of both the hole orientation  $\alpha(x,y)$  and pixel intensity  $u(x,y)$  as

$$\begin{cases} \alpha(x,y) = \frac{1}{2} \arccos\left(\frac{I_1 - I_2}{I_1 + I_2}\right) \\ u(x,y) = \frac{I_1 + I_2}{2} \end{cases}. \quad (5)$$

Using this method, we successfully realized the PDM gray scale images displayed as the Lena’s image in H state and Wang’s (the first author) image in V state, as the results shown in Fig. 3(d) and 3(c), respectively (see supplemental online material Media 2). In this case,

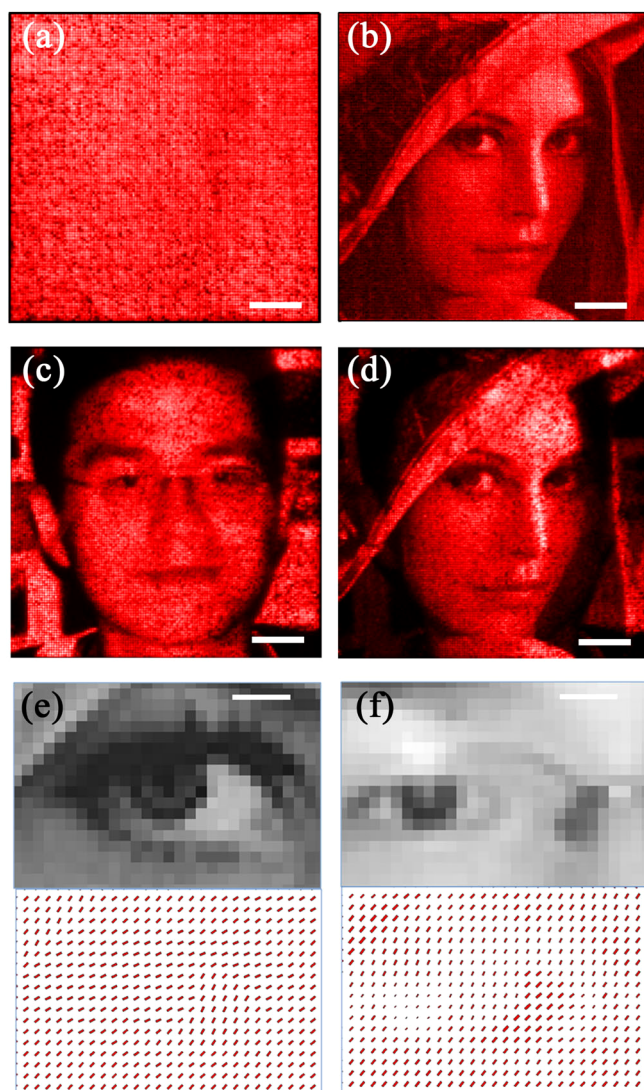


**Figure 3 | Gray scale image displays.** (a) and (b) are microscopic LED images without checking polarization and checked in H-polarization respectively for the single-image design. The portrait image in (b) corresponds to Lena, which is commonly used as a standard test image and free for the research purpose (see Ref. 13). (c) and (d) are LED images with V-polarization and H-polarization analyses respectively for the double-image sample, where the portrait in (c) belongs to Lei Wang (the first author). The permission of using this portrait has been authorized to Scientific Reports. (e) and (f) are the zoom-in images of the eye part together with the corresponding hole array designs for the single and double-image samples. Scale bar equal to 10  $\mu\text{m}$  for (a), (b), (c), and (d), 2.5  $\mu\text{m}$  for (e) and (f).

rectangular holes within the array varies both in orientation and size, as the details shown in Fig. 3(f) as the same “eye” part as in Fig. 3(e).

**Active display of dynamic patterns.** Although we have realized PDM images by the design of polarization resolved pixels, they only display static images. In principle, two PDM images actually correspond to two eigenstates of polarization (H and V) that limits its application for arbitrary animation display. However, for certain simple patterns with definite time evolutions, our design also can generate animation effects by continuously rotating the polarizer, e.g., 1D moving grating with its spatial orientation distribution defined as  $\alpha = n\pi x/L$  ( $L$  is the size of the image,  $n$  defines the number of half-period), concentric grating with  $\alpha = 8\pi\sqrt{x^2 + y^2}/L$ ,

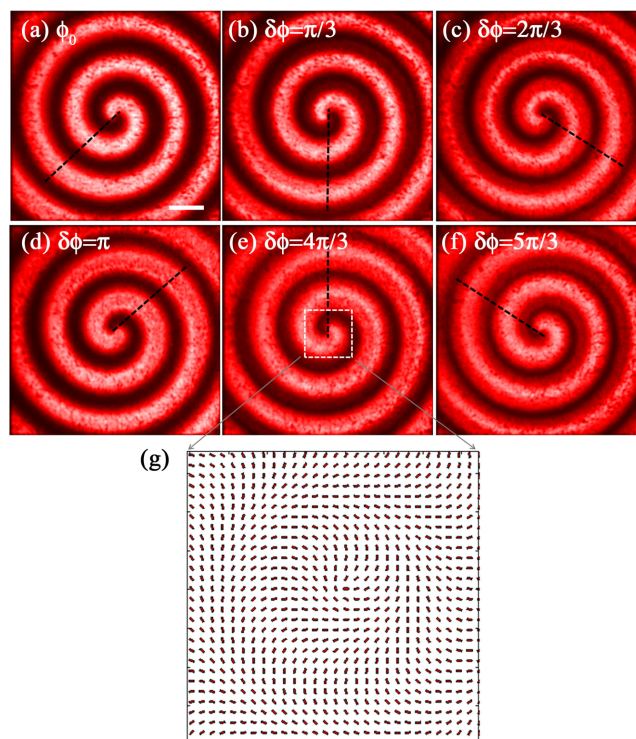


**Figure 4 | Active display for animation patterns.** (a) – (f) Microscope LED images with polarization analyses angle from 0 to  $5\pi/3$ , where black dashed lines are guiding the orientation the rotating spiral. (g) Zoom-in image of corresponding hole array design of the square area marked in (e).

and rotating vortex with  $\alpha = n\left(\theta + \frac{8\pi}{nL}\sqrt{x^2 + y^2}\right)$  ( $\theta$  is a starting angle,  $n$  is the vortex order). To visualize the animation clearly, we present the result of the rotating vortex with  $n=1$  by a series of static images in corresponding to different polarizations, as shown in Fig. 4(a)–4(f), where the dashed black line is marked to indicate the rotation. This design details of hole array is also given in Fig. 4(g) as a zoom-in image. The animation movies of this sample together with moving grating, concentric grating, and  $n=3$  rotating vortex are provided supplemental online material Media 3.

## Discussion

From the viewpoint of the display device, we have successfully achieved several kinds of the polarization tuned active images and coding, in which the PDM method is emphasized. On the other side, this kind of PDM would be also applicable in the laser illumination owing to its coherence and well defined  $k$  vectors. In those cases, by adopting a strong laser the generated dynamic image would yield strong controllable vectorial field that may work as an optical conveyor or something similar in the field of optical force. Nevertheless, what we stressed here is the integration of plasmonic polarizer on the electrically pumped LED chip, which would pave the way to really applicable nanostructured electro-optical imaging and information devices.

In summary, we proposed and realized a new integrated scheme with alliance of the EOT structure and LED chip. LED emission intensities and polarization with respect to different nanohole parameters were carefully investigated under a DC electrical supply. With well designed nano-array samples, multiplexed displays of Letter coding, gray-scale image and animations were successfully achieved by checking the polarization. Our design and results hold the significance of the compact electro-optical integration, and promise practical application the real active coding and imaging systems in microscopic region. In addition, this polarization sensitive design



can be further extended to wider areas (e. g., laser imaging, 3D display, etc.) but not limited in this electro-optical integration.

## Methods

All samples are fabricated by focus ion beam (Strata FIB 201, FEI company) milling after a 200 nm thickness silver sputtered on the LED chip (the detailed parameter of the GaAs based LED is listed in Ref. 17). Emission intensity (with a fixed wavelength at about 637 nm) of each sample was detected by an EMCCD (Andor DU888) in a microscope (Zeiss AxioImager-A1m) on the image plane by applying a bias DC current about 100 mA/cm<sup>2</sup>.

1. Ebbesen, T. W., Lezec, H. J., Ghaemi, H. F., Thio, T. & Wolff, P. A. Extraordinary optical transmission through sub-wavelength hole arrays. *Nature* **391**, 667–669 (1998).
2. Genet, C. & Ebbesen, T. W. Light in tiny holes. *Nature* **445**, 39–46 (2007).
3. Liu, H. T. & Lalanne, P. Microscopic theory of the extraordinary optical transmission. *Nature* **452**, 728–731 (2008).
4. Laux, E., Genet, C., Skauli, T. & Ebbesen, T. W. Plasmonic photon sorters for spectral and polarimetric imaging. *Nat. photonics* **2**, 161–164 (2008).
5. Inoue, D. *et al.* Polarization independent visible color filter comprising an aluminum film with surface-plasmon enhanced transmission through a subwavelength array of holes. *Appl. Phys. Lett.* **98**, 093113 (2008).
6. Koerkamp, K. J., Enoch, S., Segerink, F. B., van Hulst, N. F. & Kuipers, L. Strong influence of hole shape on extraordinary transmission through periodic arrays of subwavelength holes. *Phys. Rev. Lett.* **92**, 183901 (2004).
7. Gordon, R. *et al.* Strong polarization in the optical transmission through elliptical nanohole arrays. *Phys. Rev. Lett.* **92**, 037401 (2004).
8. van der Molen, K. L. *et al.* Role of shape and localized resonances in extraordinary transmission through periodic arrays of subwavelength holes: Experiment and theory. *Phys. Rev. B* **72**, 045421 (2005).
9. Li, T. *et al.* Zhang, X. Manipulating optical rotation in extraordinary transmission by hybrid plasmonic excitations. *Appl. Phys. Lett.* **93**, 021110 (2008).
10. Li, T., Wang, S. M., Cao, J. X., Liu, H. & Zhu, S. N. Cavity-involved plasmonic metamaterial for optical polarization conversion. *Appl. Phys. Lett.* **97**, 261113 (2010).
11. Xu, J., Li, T., Lu, F. F., Wang, S. M. & Zhu, S. N. Manipulating optical polarization by stereo plasmonic structure. *Opt. Express* **19**, 748 (2011).
12. Ellenbogen, T., Seo, K. & Crozier, K. B. Chromatic Plasmonic Polarizers for Active Visible Color Filtering and Polarimetry. *Nano Lett.* **12**, 1026–1031 (2012).

13. Kumar, K. *et al.* Printing colour at the optical diffraction limit. *Nat. Nanotechnology* **7**, 557–561 (2012).
14. Okamoto, K. *et al.* Surface-plasmon-enhanced light emitters based on InGaN quantum wells. *Nat. Mater.* **3**, 601–605 (2004).
15. Lu, Y. C. *et al.* Enhanced photoluminescence excitation in surface plasmon coupling with an InGaN/GaN quantum well. *Appl. Phys. Lett.* **91**, 183107 (2007).
16. Drezet, A. *et al.* Opening the light extraction cone of high index substrates with plasmonic gratings: Light emitting diode applications. *Appl. Phys. Lett.* **95**, 021101 (2009).
17. Wang, L. *et al.* Electrically generated unidirectional surface plasmon source. *Opt. Express* **20**, 8710–8717 (2012).

## Acknowledgements

This work is supported by the State Key Program for Basic Research of China (Nos. 2009CB930501 and 2012CB921501) and the National Natural Science Foundation of China (Nos. 10974090, 11174136, and 11021403).

## Author contributions

T.L. and S.N.Z. supervised the study. L.W. and T.L. developed design. The bare LED chip was fabricated by W.X. and X.G.X. Nanofabrication and optical measurement were carried out by L.W. theoretical modeling and calculation were performed by L.W. and R.Y.G. All the authors have analyzed and discussed the results. The manuscript was written by L.W. and T.L.

## Additional information

**Supplementary information** accompanies this paper at <http://www.nature.com/scientificreports>

**Competing financial interests:** The authors declare no competing financial interests.

**How to cite this article:** Wang, L. *et al.* Active display and encoding by integrated plasmonic polarizer on light-emitting-diode. *Sci. Rep.* **3**, 2603; DOI:10.1038/srep02603 (2013).



This work is licensed under a Creative Commons Attribution-NonCommercial-ShareAlike 3.0 Unported license. To view a copy of this license, visit <http://creativecommons.org/licenses/by-nc-sa/3.0>